Nelfinavir markedly improves lung pathology in SARS-CoV-2-infected Syrian hamsters despite a lack of an antiviral effect

Caroline S. Foo[1#], Rana Abdelnabi[1#], Suzanne J. F. Kaptein[1], Xin Zhang[1], Sebastiaan ter Horst[1], Raf Mols[2], Leen Delang[1], Joana Rocha-Pereira[1], Lotte Coelmont[1], Pieter Leyssen[1], Kai Dallmeier[1], Valentijn Vergote[1], Elisabeth Heylen[1], Laura Vangeel[1], Arnab K. Chatterjee[3], Pieter Annaert[2], Patrick Augustijns[2], Steven De Jonghe[1], Dirk Jochmans[1], Birgit Weynand[4], Johan Neyts[1*].

1. KU Leuven Department of Microbiology, Immunology and Transplantation, Rega Institute for Medical Research, Laboratory of Virology and Chemotherapy, B-3000 Leuven, Belgium.
2. KU Leuven, Department of Pharmaceutical and Pharmacological Sciences, Drug Delivery & Disposition, Box 921, 3000 Leuven, Belgium.
3. Calibr at Scripps Research, La Jolla, CA, USA.
4. KU Leuven Department of Imaging and Pathology, Translational Cell and Tissue Research, B-3000 Leuven, Belgium; Division of Translational Cell and Tissue Research.

#C.S.F. and R.A. contributed equally to this work

*To whom correspondence may be addressed. Email: johan.neyts@kuleuven.be.

Author Contributions

C.S.F., R.A., L.D., J.R.P. and J.N. designed research; C.S.F., R.A., S.J.F.K., S.T.H. R.M. and X.Z. performed research; P.A., L.D , J.R.P. and A.K.C. provided advice on the study design: C.S.F., R.A., and B.W. analyzed data; D.J., B.W. and J.N. provided advice on the interpretation of data; C.S.F., R.A.,and J.N. wrote the paper with input from co-authors; A.K.C. and S.D.J provided essential reagents; V.G. and E.H. provided and facilitated access to essential infrastructure; C.S.F., R.A.,and J.N. supervised the study; L.V., J.N., L.C., P.L. and K.D. acquired funding.

Abstract

In response to the ongoing COVID-19 pandemic, repurposing of drugs for the treatment of SARS-CoV-2 infections is being explored. The HIV protease inhibitor Nelfinavir is one of the drugs that has been shown to inhibit *in vitro* SARS-CoV2 replication. Nelfinavir is widely prescribed in combination with other HIV inhibitors. We here report on the effect of Nelfinavir in the Syrian hamster SARS-CoV-2 infection model. Although treatment of infected hamsters with either 15 or 50 mg/kg BID Nelfinavir [for four consecutive days, initiated on the day of infection] does not reduce viral RNA loads nor infectious virus titres in the lungs (as compared to the vehicle control at the end of treatment) the drug reduced virus-induced lung pathology to nearly the baseline scores of healthy animals. A substantial interstitial infiltration of neutrophils is observed in the lungs of treated (both infected and uninfected) animals. The protective effect of Nelfinavir on SARS-CoV-2-induced lung pathology (at doses that are well tolerated and that result in exposures nearing those observed in HIV-infected patients) may lay the foundation for clinical studies with this widely used drug.

Keywords

COVID-19; SARS-CoV-2; Antivirals; Nelfinavir; preclinical model.

41 **Main text**

42 The severe acute respiratory syndrome coronavirus 2 (SARS-CoV-2) resulted in more than 2.0 million
43 deaths within the time-span of a year after its discovery (1). SARS-CoV-2-induced COVID-19 is mainly
44 an inflammatory disease that displays a variety of symptoms including fever, dry cough, muscle
45 weakness, loss of sense of taste and smell, and diarrhea (2). In some patients, the disease is
46 accompanied with a massive cytokine storm and exaggerated immune response, resulting in severe
47 complications such as acute respiratory distress syndrome (ARDS), respiratory failure, septic shock and
48 multi-organ failure (2). There are no specific coronavirus antiviral drugs available to treat or prevent
49 infections with human coronaviruses. Since the *de novo* development of (a) potent specific antiviral(s)
50 for SARS-CoV-2 will take several years, repurposing of clinically approved/evaluated drugs is currently
51 adopted for rapid identification of treatment for COVID-19 (3).

52 Nelfinavir mesylate (Viracept) is an FDA-approved HIV-protease inhibitor (PI) (4). By inhibiting the HIV-
53 1 protease, it prevents the cleavage of viral Gag and Gag-Pol polyproteins, resulting in immature and
54 non-infectious virus particles (5). Nelfinavir has been reported to result in some *in vitro* inhibitory
55 activity against SARS-CoV-2. Additionally, inhibition of SARS-CoV-2 Spike glycoprotein mediated cell-
56 fusion has been reported (6) and *in silico* docking studies predict binding of Nelfinavir for the catalytic
57 site of the SARS-CoV-2 main protease, M^{pro} (7).

58 We here wanted to assess whether Nelfinavir results in antiviral effect against SARS-CoV-2 in Syrian
59 hamsters, which are highly susceptible to infection with the virus. High viral titers are reached in the
60 lung upon infection and the animals develop a COVID-like lung pathology (8). The model is well-suited
61 to assess the impact of antiviral drugs as we and others have demonstrated. Notably, we have
62 demonstrated that Favipiravir and Molnupiravir (EIDD-2801) either alone or combined, markedly
63 reduce SARS-CoV-2 replication in hamsters, whereas hydroxychloroquine does not (8, 9).

64

65 **Results**

66 Six to eight weeks female Syrian Golden hamsters were treated with Nelfinavir (15 mg/kg/dose or 50
67 mg/kg/dose) or the vehicle control by intraperitoneal injection (IP) within one hour before intranasal
68 infection with 50 µl containing $2x10^6$ $TCID_{50}$ of SARS-CoV-2 [BetaCov/Belgium/GHB-03021/2020 (EPI
69 ISL 109 72 407976|2020-02-03)] (Fig. 1A). The drug as well as the vehicle control were administered
70 twice daily for four consecutive days. At day four post-infection, lungs were collected at end-point
71 sacrifice (day 4 p.i) for viral RNA load and infectious virus titres quantification as well as lung
72 histopathology as previously described (8). Groups treated with either 15 mg/kg BID or 50 mg/kg BID
73 Nelfinavir had comparable levels of lung viral RNA load and infectious virus titres as the vehicle control
74 group (Fig. 1B, C), indicating a lack of *in vivo* antiviral efficacy of Nelfinavir in this model. Hamsters in
75 the control and 15 mg/kg BID Nelfinavir-treated groups maintained relatively stable weights
76 throughout the study, whereas a general weight loss of up to 10% was observed in the 50 mg/kg BID
77 Nelfinavir-treated group as compared to the vehicle group at 0 dpi (Fig. 1D). This weight loss can be
78 attributed to the combination of SARS-CoV-2 infection and 50 mg/kg BID Nelfinavir treatment, as this
79 dose alone did not affect the weight of two uninfected hamsters (data not shown). No other obvious
80 adverse effects were observed in either of the treatment groups. Remarkedly and intriguingly, in
81 infected animals treated with the 50 mg/kg BID Nelfinavir dose, a significant three-fold reduction in
82 the overall histological disease score compared to the placebo control was noted. In fact, the
83 histopathology score in the treated group was more or less comparable to the baseline score in
84 untreated non-infected hamsters (median score of 1.25) (Fig. 2A). Yet, despite this remarkable
85 beneficial effect on lung pathology, an unusual interstitial infiltration of neutrophils was noted in the
86 treated animals (Fig. 2A, 2B). Two uninfected hamsters treated with 50 mg/kg Nelfinavir had
87 histopathology scores at the baseline of 1 but presented as well with neutrophil infiltration (data not
88 shown), confirming that these intriguing observations are indeed attributed to Nelfinavir treatment.

89 To confirm the exposure of treated hamsters to Nelfinavir in the group treated with 50 mg/kg BID,
90 plasma levels of Nelfinavir were determined at the time of sacrifice (16h after the last treatment),
91 whereby average plasma concentrations of 174 nM were observed.

92 Taken together, although Nelfinavir does not reduce viral load in the lungs of SARS-CoV-2-infected
93 hamsters, it markedly improves lung pathology despite a massive infiltration of neutrophils.

94

95

96 **Discussion**

97 The lack of an antiviral activity of Nelfinavir against SARS-CoV2 in hamsters as observed here is
98 consistent with preliminary unpublished data in which Nelfinavir [at 250 mg/kg/day BID orally and
99 boosted with Ritonavir] had no effect on viral lung titers. However, no histopathological analysis was
100 reported (Nougairede et al., 2020 – interim report).

101 HIV PIs exert multiple effects on various cellular processes, such as reducing apoptosis of T cells and
102 neutrophils (10). In particular, Nelfinavir was reported to markedly inhibit apoptosis of neutrophils and
103 neutrophil function through inhibition of calpain (11). These findings, made in the context of HIV, are
104 consistent with our observations in Nelfinavir-treated SARS-CoV-2-infected hamsters. As part of Highly
105 Active Antiretroviral Therapy (HAART) treatment, Nelfinavir is dosed at 1250 mg BID or 750 mg TID,
106 resulting in a C_{trough} of about 370 nM measured after 12 h in patients (12). The Nelfinavir C_{trough} plasma
107 concentrations that are obtained here in hamsters with a 50 mg/kg dose at 16 hr post dosing (on
108 average 174 nM) are therefore close to or in a clinically relevant range.

109 Neutrophils extracellular traps (NETs) and matrix metalloproteinase-9 (MMP-9), which is a neutrophil-
110 released enzyme, are significantly increased in COVID-19 patients (13). Moreover, the activation of
111 NETs in COVID-19 patients was reported to correlate with disease severity and to be associated with
112 thrombo-inflammation events (13). Consequently, the inhibition of neutrophil function by Nelfinavir
113 and hence downstream immune signalling cascades may contribute to the observed reduction of SARS-
114 CoV-2-induced pathology as observed in hamsters. Furthermore, the reduction of neutrophil apoptosis
115 by the compound may account for the unusually large neutrophil infiltration observed in the lung
116 interstitium in treated animals.

117 The protective effect of Nelfinavir on SARS-CoV2 induced lung pathology as observed here, may lay
118 the foundation for clinical studies to explore whether a similar protective activity may be achieved in
119 COVID patients. In such a case that the drug would also protect patients against lung damage,
120 combination therapy with directly-acting antivirals (such as Favipiravir and Molnupiravir) against SARS-
121 CoV-2 may also be considered.

122

123 **Materials and Methods (Supporting Information)**

124 **SARS-CoV-2 strain**

125 The SARS-CoV-2 strain used in this study, BetaCov/Belgium/GHB-03021/2020 (EPI ISL 109
126 407976|2020-02-03), was recovered from a nasopharyngeal swab taken from an RT-qPCR confirmed
127 asymptomatic patient who returned from Wuhan, China in the beginning of February 2020. A close
128 relation with the prototypic Wuhan-Hu-1 2019-nCoV (GenBank accession 112 number MN908947.3)
129 strain was confirmed by phylogenetic analysis. Infectious virus was isolated by serial passaging on
130 HuH7 and Vero E6 cells (8); passage 6 virus was used for the study described here. The titer of the virus
131 stock was determined by end-point dilution on Vero E6 cells by the Reed and Muench method (14).
132 Live virus-related work was conducted in the high-containment A3 and BSL3+ facilities of the KU
133 Leuven Rega Institute (3CAPS) under licenses AMV 30112018 SBB 219 2018 0892 and AMV 23102017
134 SBB 219 20170589 according to institutional guidelines.

135 **Cells**

136 Vero E6 cells (African green monkey kidney, ATCC CRL-1586) were cultured in minimal essential
137 medium (Gibco) supplemented with 10% fetal bovine serum (Integro), 1% L- glutamine (Gibco) and 1%
138 bicarbonate (Gibco). End-point titrations were performed with medium containing 2% fetal bovine
139 serum instead of 10%.

140 **SARS-CoV-2 infection model in hamsters**

141 The hamster infection model of SARS-CoV-2 has been described before (8). In brief, wild-type Syrian
142 Golden hamsters (*Mesocricetus auratus*) were purchased from Janvier Laboratories and were housed
143 per two in ventilated isolator cages (IsoCage N Biocontainment System, Tecniplast) with ad libitum
144 access to food and water and cage enrichment (wood block). The animals were acclimated for 4 days
145 prior to study start. Housing conditions and experimental procedures were approved by the ethics
146 committee of animal experimentation of KU Leuven (license P065-2020). Female hamsters of 6-8
147 weeks old were anesthetized with ketamine/xylazine/atropine and inoculated intranasally with 50 µL
148 containing 2×10^6 TCID50 SARS-CoV-2 (day 0).

149 **Study design**

150 For D0 treatment, animals were treated twice daily with intraperitoneal injection (i.p.) of 15 mg/kg or
151 50 mg/kg of Nelfinavir (purchased from MedChem Express, formulated in 5% DMSO-5% PEG-400 and
152 5% Tween-80 in PBS to a stock of 5 mg/ml and 10 mg/ml respectively), or vehicle control (5% DMSO-
153 5% PEG-400 and 5% Tween-80) just before infection with SARS-CoV-2. Treatments continued until day

154 3 pi. During this time, hamsters were monitored for appearance, behavior, and weight. At day 4 pi,
155 hamsters were euthanized by i.p. injection of 500 µL Dolethal (200mg/mL sodium pentobarbital,
156 Vétoquinol SA). Lungs were collected and viral RNA and infectious virus were quantified by RT-qPCR
157 and end-point virus titration, respectively.

158 **SARS-CoV-2 RT-qPCR**

159 Hamster lung tissues were collected after sacrifice and were homogenized using bead disruption
160 (Precellys) in 350 µL RLT buffer (RNeasy Mini kit, Qiagen) and centrifuged (10.000 rpm, 5 min) to pellet
161 the cell debris. RNA was extracted according to the manufacturer's instructions. Of 50 µL eluate, 4 µL
162 was used as a template in RT-qPCR reactions. RT-qPCR was performed on a LightCycler96 platform
163 (Roche) using the iTaq Universal Probes One-Step RT-qPCR kit (BioRad) with N2 primers and probes
164 targeting the nucleocapsid (8). Standards of SARS-CoV-2 cDNA (IDT) were used to express viral genome
165 copies per mg tissue or per mL serum.

166 **End-point virus titrations**

167 Lung tissues were homogenized using bead disruption (Precellys) in 350 µL minimal essential medium
168 and centrifuged (10,000 rpm, 5min, 4°C) to pellet the cell debris. To quantify infectious SARS-CoV-2
169 particles, endpoint titrations were performed on confluent Vero E6 cells in 96- well plates. Viral titers
170 were calculated by the Reed and Muench method (14) using the Lindenbach calculator and were
171 expressed as 50% tissue culture infectious dose ($TCID_{50}$) per mg tissue.

172 **Histology**

173 For histological examination, the lungs were fixed overnight in 4% formaldehyde and embedded in
174 paraffin. Tissue sections (5 µm) were analyzed after staining with hematoxylin and eosin and scored
175 blindly for lung damage by an expert pathologist. The scored parameters, to which a cumulative score
176 of 1 to 3 was attributed, were the following: congestion, intra-alveolar hemorrhagic, apoptotic bodies
177 in bronchus wall, necrotizing bronchiolitis, perivascular edema, bronchopneumonia, perivascular
178 inflammation, peribronchial inflammation and vasculitis.

179 **Statistics**

180 GraphPad Prism (GraphPad Software, Inc.) was used to perform statistical analysis. Statistical
181 significance was determined using the non-parametric Mann Whitney U-test. P-values of ≤0.05 were
182 considered significant.

183

184 **Acknowledgments**

185 We thank Carolien De Keyzer, Lindsey Bervoets, Thibault Francken, Elke Maas, Jasper Rymenants, Birgit
186 Voeten, Dagmar Buyst, Niels Cremers, Bo Corbeels and Kathleen Van den Eynde for excellent technical
187 assistance. We are grateful to Piet Maes for kindly providing the SARS-CoV-2 strain used in this study.
188 We thank Jef Arnout and Annelies Sterckx (KU Leuven Faculty of Medicine, Biomedical Sciences Group
189 Management) and the Animalia and Biosafety Departments of KU Leuven for facilitating the animal
190 studies.

191

192 **References**

193 1. WHO Coronavirus Disease (COVID-19) Dashboard (February 1, 2021).

194 2. M. Z. Tay, C. M. Poh, L. Rénia, P. A. MacAry, L. F. P. Ng, The trinity of COVID-19: immunity,
195 inflammation and intervention. *Nature Reviews Immunology* **20**, 363–374 (2020).

196 3. L. Delang, J. Neyts, Medical treatment options for COVID-19. *Eur Heart J Acute Cardiovasc Care*
197 **9**, 209–214 (2020).

198 4. S. W. Kaldor, *et al.*, Viracept (Nelfinavir Mesylate, AG1343): A Potent, Orally Bioavailable
199 Inhibitor of HIV-1 Protease. *J. Med. Chem.* **40**, 3979–3985 (1997).

200 5. C. Peng, B. K. Ho, T. W. Chang, N. T. Chang, Role of human immunodeficiency virus type 1-
201 specific protease in core protein maturation and viral infectivity. *J Virol* **63**, 2550–2556 (1989).

202 6. F. Musarrat, *et al.*, The anti-HIV drug nelfinavir mesylate (Viracept) is a potent inhibitor of cell
203 fusion caused by the SARSCoV-2 spike (S) glycoprotein warranting further evaluation as an antiviral
204 against COVID-19 infections. *J Med Virol* **92**, 2087–2095 (2020).

205 7. G. Bolcato, M. Bissaro, M. Pavan, M. Sturlese, S. Moro, Targeting the coronavirus SARS-CoV-2:
206 computational insights into the mechanism of action of the protease inhibitors lopinavir, ritonavir and
207 nelfinavir. *Scientific Reports* **10**, 20927 (2020).

208 8. S. J. F. Kaptein, *et al.*, Favipiravir at high doses has potent antiviral activity in SARS-CoV-2-
209 infected hamsters, whereas hydroxychloroquine lacks activity. *Proc Natl Acad Sci U S A* **117**, 26955–
210 26965 (2020).

211 9. R. Abdelnabi, *et al.*, Molnupiravir (EIDD-2801) inhibits SARS-CoV2 replication in Syrian
212 hamsters model. *bioRxiv*, 2020.12.10.419242 (2020).

213 10. C. M. Mastroianni, *et al.*, Ex Vivo and In Vitro Effect of Human Immunodeficiency Virus Protease
214 Inhibitors on Neutrophil Apoptosis. *The Journal of Infectious Diseases* **182**, 1536–1539 (2000).

215 11. N. Hadad, R. Levy, F. Schlaeffer, K. Riesenberg, Direct effect of human immunodeficiency virus
216 protease inhibitors on neutrophil function and apoptosis via calpain inhibition. *Clin Vaccine Immunol*
217 **14**, 1515–1521 (2007).

218 12. M. Regazzi, *et al.*, Clinical Pharmacokinetics of Nelfinavir and Its Metabolite M8 in Human
219 Immunodeficiency Virus (HIV)-Positive and HIV-Hepatitis C Virus-Coinfected Subjects. *Antimicrobial*
220 *Agents and Chemotherapy* **49**, 643 LP – 649 (2005).

221 13. E. Petito, *et al.*, Neutrophil more than platelet activation associates with thrombotic
222 complications in COVID-19 patients. *J Infect Dis* (2020) https:/doi.org/10.1093/infdis/jiaa756.

223 14. L. J. Reed, H. Muench, A simple method of estimating fifty percent endpoints. *The american*
224 *journal of hygiene* **27**, 493–497 (1938).

225

226

227

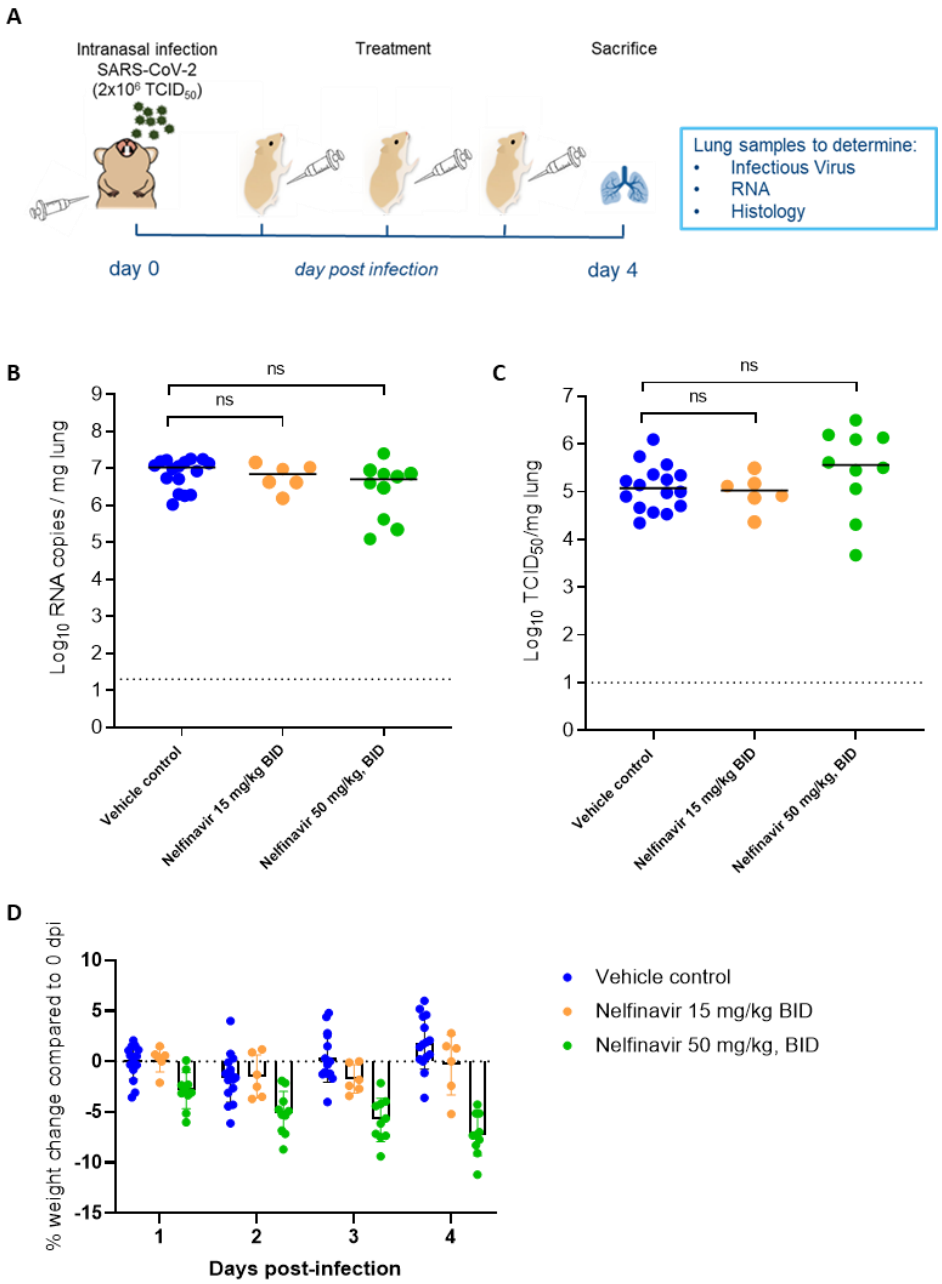

Fig. 1. **Nelfinavir does not reduce viral replication in SARS-CoV-2 infected hamsters. (A)** Set-up of the study. **(B)** Viral RNA levels in the lungs of hamsters treated with vehicle (control), 15 mg/kg Nelfinavir BID, or 50 mg/kg Nelfinavir BID at 4 dpi expressed as $\log_{10}$ SARS-CoV-2 RNA copies per mg lung tissue. Individual data and median values are presented. **(C)** Infectious virus titers in the lungs of hamsters treated with vehicle (control), 15 mg/kg Nelfinavir BID, or 50 mg/kg Nelfinavir BID at 4 dpi expressed as $\log_{10}$ $TCID_{50}$ per mg lung tissue. Individual data and median values are presented. **(D)** Daily weight change in percentage, normalized to the body weight at the time of infection. Bars represent average ± SD. All data (panels B, C, D) are from one (for 15 mg/kg dose) to two independent experiments with

237 a total of 16, 6, and 10 animals for the placebo, 15 mg/kg, and 50 mg/kg conditions respectively. Data
238 were analyzed with the Mann-Whitney U test. ns, non-significant.

239

240

A

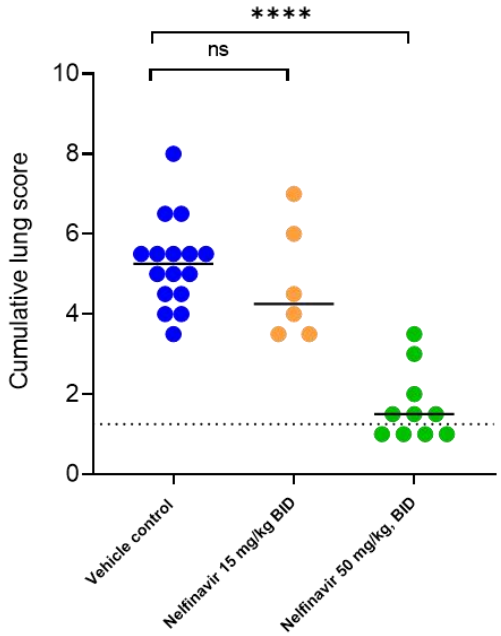

B

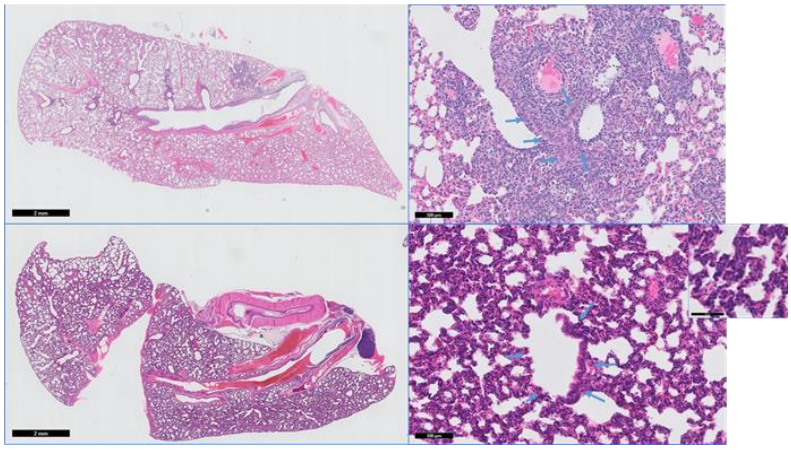

Figure 2. Nelfinavir markedly improves lung pathology of SARS-CoV-2-infected Syrian hamsters despite interstitial neutrophil infiltration. (A) Cumulative severity score from H&E-stained slides of lungs from vehicle control and Nelfinavir (50 mg/kg BID)-treated SARS-CoV-2-infected hamsters at 4 dpi. Individual datapoints and lines indicating median values are presented. The dotted line represents the median lung score in healthy untreated non-infected animals. Data were analyzed using the Mann-Whitney U test. ****P<0.0001. (B) Representative H&E-stained slides of lungs from vehicle control (top panels) and Nelfinavir-treated (bottom panels) SARS-CoV-2-infected hamsters at 4 dpi. Top, left: peri-bronchial inflammation and bronchopneumonia in vehicle-treated hamsters. Top, right: higher magnification of bronchopneumonia centred on a bronchiol (blue arrows) in vehicle-treated hamsters. Bottom, left: dark blue-stained interstitium and bronchial structures appearing normal without inflammation in Nelfinavir-treated hamsters. Bottom, right: severe interstitial inflammation with mostly PMN and congestion. Blue arrows indicate bronchiol (Insert at higher magnification).